BioChip J. (2017) 11(1): 46-56
DOI 10.1007/s13206-016-1107-6

Original Article

Glucose Detection Using 4-mercaptophenyl Boronic Acid-incorporated Silver Nanoparticles-embedded Silica-coated Graphene Oxide as a SERS Substrate

Xuan-Hung Pham[1], Seongbo Shim[1], Tae-Han Kim[1], Eunil Hahm[1], Hyung-Mo Kim[1], Won-Yeop Rho[1], Dae Hong Jeong[2], Yoon-Sik Lee[3] & Bong-Hyun Jun[1,*]

Received: 18 May, 2016 / Accepted: 18 August, 2016 / Published online: 07 September, 2016

Abstract In this work, 4-mercaptophenyl boronic acid (4-MPBA) was self-assembled on the surface of silver nanoparticle-embedded silica-coated graphene oxide (GO@SiO_2@Ag NPs@MPBA) to detect glucose by surface enhanced Raman scattering (SERS). The SERS intensity of 4-MPBA on the GO@SiO_2@Ag NPs was 2.2-fold greater than that of GO@Ag NPs. Moreover, silica-coated GO exhibited lower background signals compared to GO. The SERS intensity of GO@SiO_2@Ag NPs@MPBA peaked at 1 mM 4-MPBA. pH-dependent behavior of 4-MPBA on the GO@SiO_2@Ag NPs was investigated; the highest SERS signal intensity was detected at pH 3. The binding of glucose to 4-MPBA-incorporated GO@SiO_2@Ag NPs increased the SERS signals at both 1,072 and 1,588 cm^{-1}. The linear range was estimated from 2 to 20 mM glucose. These results provide insight into detection of glucose and the development of SERS-based biosensors using graphene oxide.

Keywords: Glucose detection, Graphene oxide, Silica coating, SERS, Signal enhancement

[1]Department of Bioscience and Biotechnology, Konkuk University, Seoul 05029, Republic of Korea
[2]Department of Chemistry Education, Seoul National University, Seoul 08826, Republic of Korea
[3]School of Chemical and Biological Engineering, Seoul National University, Seoul 08826, Republic of Korea
*Correspondence and requests for materials should be addressed to B.-H. Jun (✉bjun@konkuk.ac.kr)

Introduction

Monitoring of glucose concentration is important in the care of diabetes[1-7]. Various methods for glucose detection have been reported, including colorimetric detection[8-12], electrochemical detection[13-15], fluorescence detection[16-18] and Raman spectroscopy[19-22]. Compared to these techniques, surface-enhanced Raman scattering (SERS) has several advantages, such as ultrahigh sensitivity, selectivity and *in vivo* application[23-25]. However, the low affinity of glucose for bare metal surfaces and the low Raman scattering cross-section of polarizability of glucose limits detection by SERS[19,26,27]. To achieve a high affinity and selectivity for glucose, a broad range of boronic acid-based Raman reporters have been synthesized to capture glucose selectively on the substrate[19,21,26-31]. Most of these studies focused on the specific binding of glucose to the boronic acid motif in 4-mercaptophenyl boronic acid (4-MPBA), which resulted in a significant increase in the absolute intensity of the SERS signal of MPBA due to an orientation change and the charge transfer effect. An active SERS substrate composed of a silver nanorod with a 4-MPBA monolayer was reported for quantitative detection of glucose[19]. However, the preparation of silver nanorods by physical vapor deposition can be complicated and can limit their applications. The SERS behaviors of 4-MPBA incorporated on assembled Ag NPs in various media, which may lead to the properties of the functional molecules being different from those in a solution, were also reported[20]. It was demonstrated that the association of OH^- with MPBA might lead to

the self-condensation of MPBA to form an anhydride, which may, in turn, affect the binding of glucose through the formation of esters. Also, a properly designed SERS detection strategy was proposed to eliminate the spectral interference from the similarity between the SERS spectra of D-glucose-associated MPBA and OH^--associated MPBA species. However, calculation of the peak area was complicated and the linear range of glucose concentration was limited.

Graphene and graphene oxide (GO) are promising SERS substrates due to their ability to generate strong chemical enhancement[32-36]. Compared with graphene, GO can be produced at a high yield and low cost, which facilitates its practical application[37-47]. However, the chemical enhancement of GO itself displays low sensitivity. To overcome this issue, composites that combine the advantages of GO with the high electromagnetic enhancement of gold or silver nanoparticles (Au or Ag NPs) have been developed for SERS detection[48-54]. Metal NPs were deposited on the surface of GO at sites of oxygen-containing functional groups, such as carbonyl and hydroxyl groups[55,56]. Two-component graphene-metals as SERS substrates have also been reported, but few have evaluated ternary component hybrids for SERS analysis, which may have additional advantages, such as higher sensitivity, easy separation, and a concentration effect. Recently, we developed a novel hybrid silver nanoparticle-embedded thin silica-coated GO structure (GO@SiO_2@Ag NPs), which enhances the SERS signal, as a SERS substrate.

In this study, 4-MPBA was incorporated on the surface of GO@SiO_2@Ag NPs (GO@SiO_2@Ag NPs@MPBA) to detect glucose by SERS. The SERS intensity of 4-MPBA on GO@SiO_2@Ag NPs and GO@Ag NPs was compared. The optimal conditions in terms of generating the maximum SERS signal intensity of GO@SiO_2@Ag NPs@MPBA were determined. Moreover, the pH-dependent behavior of 4-MPBA on GO@SiO_2@Ag NPs was investigated, and the ability of GO@SiO_2@Ag NPs@MPBA to detect glucose was evaluated.

Results and Discussion

Preparation of Ag NPs-embedded Silica-coated GO

4-Mercaptophenylboronic acid (4-MPBA) incorporated Ag NPs-embedded silica-coated GO (GO@SiO_2@Ag NPs@MPBA) was prepared for detection of glucose, as shown in Figure 1a). Ag NPs-embedded silica-coated GO (GO@SiO_2@Ag NPs) was prepared using the method reported by our group (see Supporting Figure). Briefly, first, GO@SiO_2 was prepared by coating a thin silica shell on the surface of GO through physical adsorption of sodium silicate (see Supporting Figure S1)[57]. GO@SiO_2 was functionalized with thiol groups, which have strong affinity for Ag, using 3-mercaptopropyl trimethoxysilane (MPTS). Then, Ag NPs were embedded on the surface of the thiolated GO@SiO_2. Here, GO@SiO_2 was used as a carrier template to enhance the SERS. Finally, GO@SiO_2@Ag NPs was incubated with 1 mM 4-MPBA to incorporate 4-MPBA on its surface by means of the affinity of thiol groups for silver.

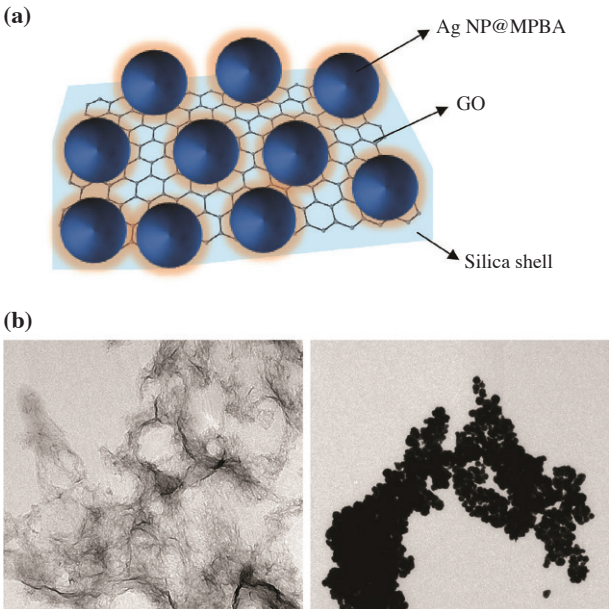

Figure 1. (a) Structure of silver nanoparticle-embedded silica-coated graphene oxide (GO@SiO_2@Ag NPs) and (b) TEM images of graphene oxide (GO) and GO@SiO_2@Ag NPs.

Figure 1b shows TEM images of GO and GO@SiO_2@Ag NPs. Due to agglomeration of GO sheets[58], GO was wrinkled and transparent. After coating with a thin layer of silica and embedding of Ag NPs, the surface of GO@SiO_2@Ag NPs was fully covered with Ag NPs.

To confirm the presence of a silica layer on the surface of GO, energy-dispersive X-ray spectroscopy (EDS) of sodium silicate-coated GO and thiolated GO@SiO_2 was performed (Figure S2). The atomic composition of sodium silicate-coated GO was 5.5%, 62.0%, 25.3% and 7.2% C, O, Si, Na, respectively (Figure S2a). After deposition of MPTS on GO, the C and Si contents increased to 8.0% and 30.9% while that of O decreased slightly to 58.3% (Figure S2b). The presence of 0.3% S confirmed the successful deposition of MPTS on GO@SiO_2.

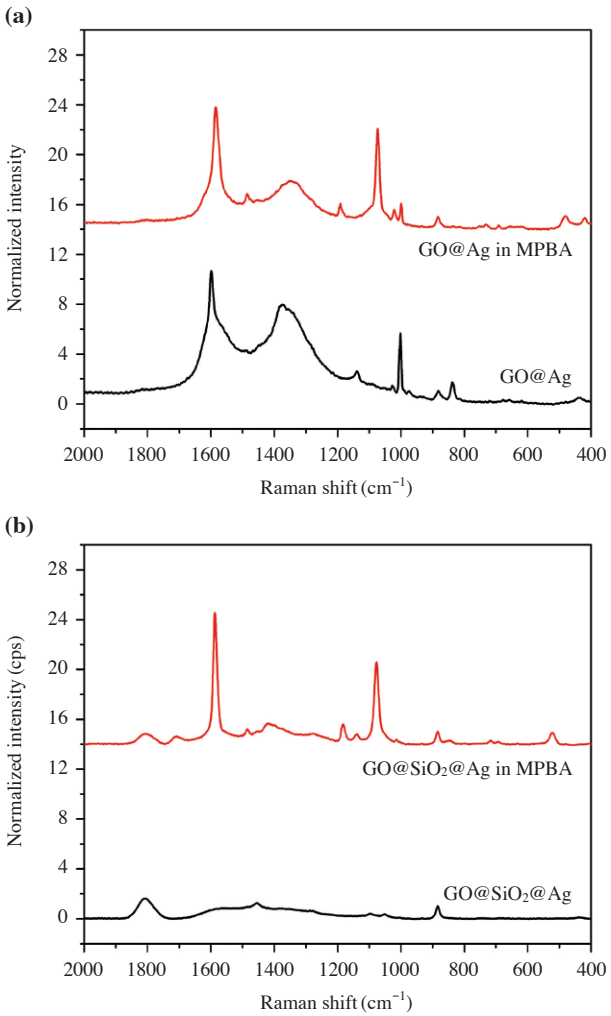

Figure 2. SERS spectra of (a) GO@SiO_2@Ag NPs and (b) GO@Ag NPs in EtOH solution with and without 1 mM 4-mercaptophenylboronic acid (4-MPBA). GO concentration was 1 mg/mL, laser power was 10 mW, wavelength was 532 nm, integration time was 5 s, and laser spot size was 2 μm.

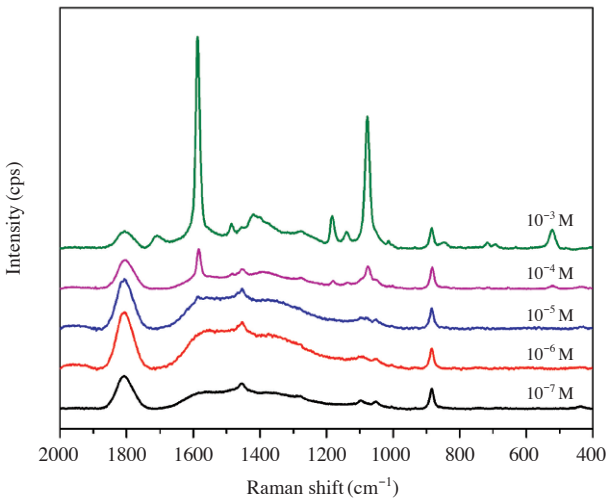

Figure 3. SERS spectra of GO@SiO_2@Ag NPs with 4-MPBA concentrations of 1×10^{-3} to 1×10^{-7} M in EtOH solution. Laser power was 10 mW, wavelength was 532 nm, integration time was 5 s, and laser spot size was 2 μm.

SERS Activity of GO@SiO_2@Ag NPs toward 4-mercaptophenylboronic Acid

The SERS activity of GO@SiO_2@Ag NPs was investigated using 4-mercaptophenylboronic acid (4-MPBA) as a SERS substrate. The boronic acid group of 4-MPBA exhibits a strong and selective affinity for glucose, and the specific binding of glucose to the boronic acid in 4-MPBA resulted in a significant increase in the absolute intensity of the SERS signal of MPBA due to an orientation change and the charge transfer effect[19]. In addition, the benzene ring containing a thiol group facilitated assembly on the surface of Ag NPs and functioned as a Raman reporter to determine the SERS signal. The Raman signals were recorded using a micro Raman system in a capillary tube. Figure 3 shows the SERS spectra of GO@Ag NPs in EtOH solution in the presence and absence of 1 mM 4-MPBA. In the absence of 4-MPBA, typical broad peaks at ~1,342 cm^{-1} and 1,595 cm^{-1}, which corresponded to the D and G peaks, respectively, were evident in GO@Ag NPs[33,59]. In the presence of 1 mM 4-MPBA, GO@Ag NPs showed the typical Raman spectrum of 4-MPBA with dominant peaks at ~1,073 and ~1,584[60,61]. The peak at 1,073 cm^{-1} was attributed to ring C-C bending and C-S stretching and the peak at 1,584 cm^{-1} was assigned to ring C-C stretching[62]. The SERS spectrum of GO@SiO_2@Ag NPs in EtOH solution in the presence of 1 mM 4-MPBA was similar to that of GO@Ag NPs. However, the D and G peaks of GO at ~1,342 cm^{-1} and 1,595 cm^{-1} were unclear due to the silica layer coating. Also, the peaks at 1,073 and 1,584 cm^{-1} were shifted to 1,077 and 1,587 cm^{-1}, respectively. Interestingly, the SERS intensity of GO@SiO_2@Ag NPs in the absence of 4-MPBA was dramatically decreased compared to that of GO@Ag. This indicated that the silica coating reduced the background signals from GO and enhances the limit of detection. Also, the SERS signal of the GO@SiO_2@Ag NPs at 1,077 cm^{-1} was ~1,069 ± 265 cps with 1 mM 4-MPBA, and was 1.8-fold greater than that of GO@Ag NPs (597 ± 54 cps). Similarly, the SERS intensity of GO@SiO_2@Ag NPs at 1,588 cm^{-1} was 2.2-fold greater than that of GO@Ag NPs (726 ± 75 cps). This is due to the effect of the average size and density of Ag NPs on the surface of GO or GO@SiO_2. That is, Ag NPs on thin-silica-coated GO have

a higher density than those on non-silica-coated GO. Furthermore, the thin silica shell allowed 4-MPBA to close to the GO@SiO_2@Ag NPs, which enhanced the SERS signal both from Ag NPs to Ag NPs and from Ag NPs to the GO platform[63].

The SERS intensity of GO@SiO_2@Ag NPs was next examined in the presence of various concentrations of 4-MPBA. The SERS signals at 1×10^{-3} - 1×10^{-7} M4-MPBA confirmed that the SERS intensity of GO@SiO_2@Ag NPs increased with 4-MPBA concentration and peaked at 1×10^{-3} M 4-MPBA. In particular, the intensities of the Raman bands at 1,077 and 1,584 cm^{-1} increased dramatically with 4-MPBA concentration.

Glucose Detection Using 4-MPBA Incorporated GO@SiO_2@Ag NPs

Optimal Conditions for Glucose Detection

Before application of GO@SiO_2@Ag NPs@MPBA to the detection of glucose, several influencing factors were considered, including the pH of the sensing system and incubation time. The boronic acid group in 4-MPBA is sensitive to the pH value and affected the tilted orientation of the 4-MPBA molecules adsorbed on the surface of GO@SiO_2@Ag NPs. The SERS spectra of MPBA molecules on the Ag NPs were examined in solutions with different pH values. To prevent the formation of boronic acid anhydride from self-condensation of 4-MPBA under basic conditions[20], the pH value of the solution was controlled in the range pH 1.0 to 9.0 (Figure 4 and Figure S3-S8). In the absence of glucose, the SERS intensity of the CC stretching at ~1,587 cm^{-1} and the CCC bending at ~1,073 cm^{-1} increased from pH 1.0 to pH 3.0 and decreased at higher pH values. However, the pH value exerted a significant effect on the Raman shift. At pH <1.0, CC stretching was located at 1,588 cm^{-1} (Figure S3), indicating that 4-MPBA remained in the original form with a B atom with sp^2-hybridization. At pH ≥ 5.0, a new band at 1,573 cm^{-1} appeared due to the presence of OH^- will converse the original 4-MPBA (-$B(OH_2)$) to an OH^--associated 4-MPBA form (-$B(OH)_3^-$). Similar pH-dependent behavior of the CC stretching mode has been reported for 4-MPBA-assembled Ag NPs[19,20]. Also, the intensity of in-plane CH and CCC bending modes at 1,021 and 988 cm^{-1} became distinct and stronger at pH 3.0. The intensities of these two bands decreased at pH values >3.0. The out-of-plane modes of CCC bending and CH bending at 752 cm^{-1} and 473 cm^{-1} increased in intensity moderately. Similarly, the out-of-plane modes of CCC and CH bending weakened at pH >3.0. In the presence of glucose, the SERS intensity increased and peaked at pH 3.0. pH >3.0 led

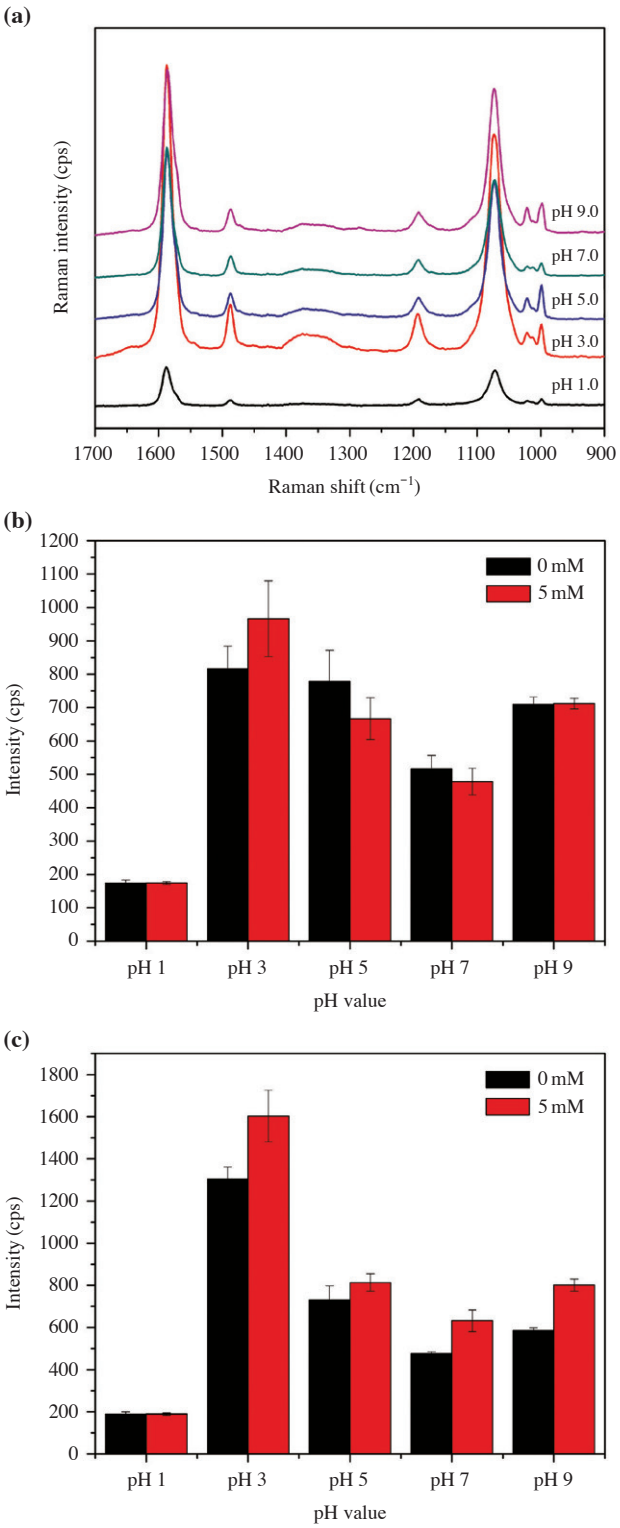

Figure 4. (a) SERS spectra of 4-MPBA incorporated GO@SiO_2@Ag NPs in the presence of 5 mM glucose at various pH values. SERS intensities were at (b) 1,073 cm^{-1} and (c) 1,588 cm^{-1} of 4-MPBA incorporated GO@SiO_2@Ag NPs in the absence and presence of 5 mM glucose at various pH values. Incubation time was fixed at 30 min.

to a decrease in SERS intensity. Under acidic conditions, the Raman shifts were non-significantly changed compared with those in the absence of glucose. At pH ≥ 5, the CC stretching mode at 1,586 cm^{-1} (original 4-MPBA) was shifted to 1,584 cm^{-1} in the presence of glucose. In contrast, the intensity of the Raman peak at 1,573 cm^{-1} (OH^- associated 4-MPBA) decreased, leading the relative intensity of 1,584 and 1,573 cm^{-1} to increase. For example, the relative intensity of 1,584 and 1,573 cm^{-1} at pH 5.0 was 1.92 but it increased to 2.74 at pH 7.0.

The effect of incubation time from 10 to 120 min was also examined (Figure S9). After 10 min, the SERS intensity stabilized. Further increases in incubation time did not affect on the SERS intensity significantly, indicating that glucose required a short period to bind with 4-MPBA on the surface of @GO@SiO_2@Ag NPs@MPBA.

Glucose Detection of 4-MPBA Incorporated GO@SiO_2@Ag NPs

4-MPBA incorporated GO@SiO_2@Ag NPs was used as an active SERS substrate under the optimal conditions for detection of glucose in PBS. The 4-MPBA incorporated GO@SiO_2@Ag NPs were mixed with various concentrations of glucose and the sensing ability evaluated (Figure 5). Since glucose has a low affinity for silver and low Raman scattering cross-section of polarizability of glucose, it did not yield any peaks. The strong SERS signals shown in Figure 5 belong to 4-MPBA. However, the SERS intensity of 4-MPBA on the surface of GO@SiO_2@Ag NPs increased with increasing glucose concentration in the range 2×10^{-3} - 20×10^{-3} M. This result confirmed that GO@SiO_2@Ag NPs@MPBA can be used as a substrate to detect glucose. Specifically, the intensities of the Raman bands at 1,072 and 1,588 cm^{-1} increased as the glucose concentration increased. Figure 5b shows the correlation between peak intensity and glucose concentration. The linear range of glucose concentration from 2 to 20 mM indicates that our material is sufficiently sensitive for detecting glucose in blood.

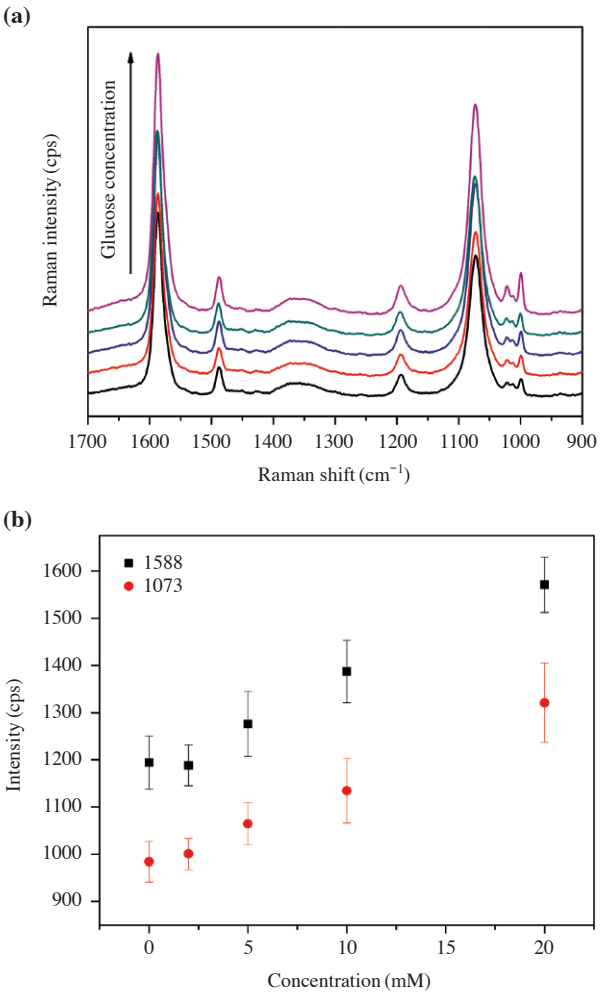

Figure 5. (a) SERS spectra and (b) calibration curves of GO@SiO_2@Ag NPs according to glucose concentration in PBS buffer (pH 3.0). Incubation time was fixed at 10 min.

Conclusions

In summary, 4-mercaptophenylboronic acid-assembled silver NP-assembled silica-coated graphene oxide (GO@SiO_2@Ag NPs) was prepared by introducing 4-MPBA onto the Ag NPs of silica-coated graphene oxide. This was used to assay glucose based on the affinity of boronic acid group and glucose. The SERS intensity of 4-MPBA on GO@SiO_2@Ag NPs was 2.2-fold greater than that of GO@Ag NPs. Interestingly, silica-coated GO exhibited lower background signals compared to GO. The SERS intensity of GO@SiO_2@Ag NPs@MPBA peaked at 1 mM 4-MPBA. The pH-dependent behavior of 4-MPBA on GO@SiO_2@Ag NPs was also investigated. The binding of glucose to 4-MPBA incorporated GO@SiO_2@Ag NPs increased the intensity of the SERS signals at 1,072 and 1,588 cm^{-1}. The linear range was estimated to be from 2 to 20 mM glucose. These results provide new insight into the development of SERS-based biosensors using graphene oxide as a substrate.

Materials and Methods

Tetraethylorthosilicate (TEOS), 3-mercaptopropyl tri-

methoxysilane (MPTS), ethylene glycol (EG), silver nitrate ($AgNO_3$, 99.99%), octylamine (OA), sodium silicate solution, D-glucose and 4-mercaptophenylboronic acid (4-MPBA) were purchased from Sigma-Aldrich (St. Louis, MO, USA) and used without further purification. Nano graphene oxide (GO) was purchased from Graphene Supermarket (Calverton, New York, USA). Ethyl alcohol and aqueous ammonium hydroxide (NH_4OH, 27%) were purchased from Daejung (Siheung, Korea).

Preparation of Silver Nanoparticle-embedded Silica Coated Graphene Oxide (GO@SiO_2@Ag NPs)

GO (6 mg) was dispersed into 15 mL water, and 15 μL sodium silicate solution (0.036 wt%) was added and stirred vigorously for 12 h at 25°C. Silica-coated GO was centrifuged at 12000 × g for 30 min and washed several times with ethanol. GO@SiO_2 (3 mg) was dispersed into 10 mL EtOH. Then, 10 μL of MPTS and 40 μL of NH_4OH were added to the solution and stirred vigorously for 6 h at 25°C. GO@SiO_2 was obtained by centrifugation at 12000 × g for 30 min and washed several times with ethanol. Ag NPs were introduced to the surface of GO@SiO_2 by a method developed in our laboratory with some modifications[64,65]. Briefly, GO@SiO_2 (2 mg) was first dissolved in 10 mL EG, and 10 mL $AgNO_3$ solution (1 mg/mL in EG) was added to GO@SiO_2 solution and mixed thoroughly. Octylamine (41.3 μL) was added and the resulting suspension was stirred for 6 h at 25°C. The particles were centrifuged at 5000 × g for 15 min and washed several times with ethanol. For comparison, GO without a silica coating was used as a control. Ag NPs were introduced onto the surface of GO using the aforementioned procedure. Silver nanoparticle-embedded graphene oxide was termed GO@Ag NP.

Incorporation of 4-mercaptophenylboronic Acid (4-MPBA) in GO@SiO_2@Ag NPs

4-MPBA in EtOH (1 mM; 1 mL) was added to 1 mg of GO@SiO_2@Ag NPs or GO@Ag NPs. The suspension was incubated for 1 h at 25°C. The colloids were then centrifuged and washed five times with EtOH. The materials were redispersed in EtOH to obtain 4-MPBA-incorporated GO@SiO_2@Ag or 4-MPBA-incorporated GO@Ag solution (1 mg/mL).

Glucose Detection Using GO@SiO_2@Ag NPs@MPBA

In general, glucose in 10 mM PBS buffer (pH 3.0) containing 1 mg/mL PVP was added to GO@SiO_2@Ag@MPBA and incubated for 30 min at 25°C. This solution was assayed using a micro-Raman system (LabRam 300, JY-Horiba, Tokyo, Japan).

SERS Measurement

To evaluate their sensitivity, the synthesized SERS materials were transferred into capillary tubes and assayed by a micro-Raman system (LabRam 300, JY-Horiba, Tokyo, Japan) equipped with an optical microscope (BX41, Olympus, Japan). The SERS signals were collected in a back-scattering geometry using a ×10 objective lens (0.90 NA, Olympus, Japan) and detected by a spectrometer equipped with a thermoelectric-cooled CCD detector. As a photo-excitation source, a 532 nm diode-pumped solid-state laser (CL 532-100-S, Crystalaser, USA) was used with a laser power of 10 mW at the sample. The strong Rayleigh scattered light was rejected using a long-pass filter. Selected sites were measured randomly, and all SERS dot spectra were integrated for 5 s.

Acknowledgements Consulting service from the Microbial Carbohydrate Resource Bank (MCRB, Seoul, Korea) was kindly appreciated. This research was supported by the Basic Science Research Program through the National Research Foundation of Korea (NRF) funded by the Ministry of Science, ICT & Future Planning (2016-A002-0048) and by the Bio & Medical Technology Development Program of the National Research Foundation (NRF) & funded by the Korean government (MSIP&MOHW) (2016-A423-0045).

References

1. Reach, G. & Wilson, G.S. Can Continuous Glucose Monitoring Be Used for the Treatment of Diabetes. *Anal. Chem.* **64**, 381A-386A (1992).
2. Kim, H. *et al*. TRAMP Prostate Tumor Growth Is Slowed by Walnut Diets Through Altered IGF-1 Levels, Energy Pathways, and Cholesterol Metabolism. *J. Med. Food* **17**, 1281-1286 (2014).
3. Ban, J.O. *et al*. Antiobesity Effects of a Sulfur Compound Thiacremonone Mediated via Down-regulation of Serum Triglyceride and Glucose Levels and Lipid Accumulation in the Liver of db/db Mice. *Phytother. Res.* **26**, 1265-1271 (2012).
4. Shin, K.C. *et al*. Highly selective hydrolysis for the outer glucose at the C-20 position in ginsenosides by beta-glucosidase from Thermus thermophilus and its application to the production of ginsenoside F-2 from gypenoside XVII. *Biotechnol. Lett.* **36**, 1287-1293 (2014).
5. Lee, H.J. *et al*. Production of aglycone protopanaxatriol from ginseng root extract using Dictyoglomus

turgidum beta-glycosidase that specifically hydrolyzes the xylose at the C-6 position and the glucose in protopanaxatriol-type ginsenosides. *Appl. Microbiol. Biotechnol.* **98**, 3659-3667 (2014).
6. Shin, K.C. & Oh, D.K. Characterization of a novel recombinant beta-glucosidase from Sphingopyxis alaskensis that specifically hydrolyzes the outer glucose at the C-3 position in protopanaxadiol-type ginsenosides. *J. Biotechnol.* **172**, 30-37 (2014).
7. Bae, S. *et al*. Neutrophil Proteinase 3 Induces Diabetes in a Mouse Model of Glucose Tolerance. *Endocr. Res.* **37**, 35-45 (2012).
8. Musto, C.J. & Suslick, K.S. Differential sensing of sugars by colorimetric arrays. *Curr. Opin. Chem. Biol.* **14**, 758-766 (2010).
9. Deng, J. *et al*. Visualization and Quantification of Neurochemicals with Gold Nanoparticles: Opportunities and Challenges. *Adv. Mater.* **26**, 6933-6943 (2014).
10. Radhakumary, C. & Sreenivasan, K. Naked Eye Detection of Glucose in Urine Using Glucose Oxidase Immobilized Gold Nanoparticles. *Anal. Chem.* **83**, 2829-2833 (2011).
11. Jiang, Y. *et al*. Colorimetric Detection of Glucose in Rat Brain Using Gold Nanoparticles. *Angew. Chem., Int. Ed.* **49**, 4800-4804 (2010).
12. Li, C. *et al*. Stimuli-Triggered Off/On Switchable Complexation between a Novel Type of Charge-Generation Polymer (CGP) and Gold Nanoparticles for the Sensitive Colorimetric Detection of Hydrogen Peroxide and Glucose. *Macromolecules* **44**, 429-431 (2011).
13. Takahashi, S. & Anzai, J.-i. Phenylboronic Acid Monolayer-Modified Electrodes Sensitive to Sugars. *Langmuir* **21**, 5102-5107 (2005).
14. Li, J. *et al*. A sensitive non-enzyme sensing platform for glucose based on boronic acid-diol binding. *Sens. Actuators, B* **161**, 832-837 (2012).
15. Gao, P. *et al*. A glucose-responsive pH-switchable bioelectrocatalytic sensor based on phenylboronic acid-diol specificity. *Electrochim. Acta* **151**, 370-377 (2015).
16. Zhang, L. *et al*. Boron-Doped Graphene Quantum Dots for Selective Glucose Sensing Based on the "Abnormal" Aggregation-Induced Photoluminescence Enhancement. *Anal. Chem.* **86**, 4423-4430 (2014).
17. Wannajuk, K. *et al*. Highly specific-glucose fluorescence sensing based on boronic anthraquinone derivatives via the GOx enzymatic reaction. *Tetrahedron* **68**, 8899-8904 (2012).
18. Yan, J. *et al*. Boronolectins and fluorescent boronolectins: An examination of the detailed chemistry issues important for the design. *Med. Res. Rev.* **25**, 490-520 (2005).
19. Sun, X. *et al*. Functionalized aligned silver nanorod arrays for glucose sensing through surface enhanced Raman scattering. *RSC Adv.* **4**, 23382-23388 (2014).
20. Li, S. *et al*. Surface-enhanced Raman scattering behaviour of 4-mercaptophenyl boronic acid on assembled silver nanoparticles. *Phys. Chem. Chem. Phys.* **17**, 17638-17645 (2015).
21. Torul, H. *et al*. Glucose determination based on a two component self-assembled monolayer functionalized surface-enhanced Raman spectroscopy (SERS) probe. *Anal. Methods* **6**, 5097-5104 (2014).
22. Gupta, V.K. *et al*. A novel glucose biosensor platform based on Ag@AuNPs modified graphene oxide nanocomposite and SERS application. *J. Colloid Interface Sci.* **406**, 231-237 (2013).
23. Harper, M.M. *et al*. Recent developments and future directions in SERS for bioanalysis. *Phys. Chem. Chem. Phys.* **15**, 5312-5328 (2013).
24. Gong, X. *et al*. Individual nanostructured materials: fabrication and surface-enhanced Raman scattering. *Chem. Commun.* **48**, 7003-7018 (2012).
25. Hahm, E. *et al*. β-CD dimer-immobilized Ag assembly embedded silica nanoparticles for sensitive detection of polycyclic aromatic hydrocarbons. *Sci. Rep.* **6**, 26082 (2016).
26. Shafer-Peltier, K.E. *et al*. Toward a Glucose Biosensor Based on Surface-Enhanced Raman Scattering. *JACS* **125**, 588-593 (2003).
27. Lyandres, O. *et al*. Progress Toward an In Vivo Surface-Enhanced Raman Spectroscopy Glucose Sensor. *Diabetes Technol. Ther.* **10**, 257-265 (2008).
28. Bull, S.D. *et al*. Exploiting the Reversible Covalent Bonding of Boronic Acids: Recognition, Sensing, and Assembly. *Acc. Chem. Res.* **46**, 312-326 (2013).
29. Hansen, J.S. *et al*. Arylboronic acids: A diabetic eye on glucose sensing. *Sens. Actuators, B* **161**, 45-79 (2012).
30. Nishiyabu, R. *et al*. Boronic acid building blocks: tools for sensing and separation. *Chem. Commun.* **47**, 1106-1123 (2011).
31. Ye, J. *et al*. A Boronate Affinity Sandwich Assay: An Appealing Alternative to Immunoassays for the Determination of Glycoproteins. *Angew. Chem., Int. Ed.* **53**, 10386-10389 (2014).
32. Ling, X. *et al*. Can Graphene be used as a Substrate for Raman Enhancement? *Nano Lett.* **10**, 553-561 (2010).
33. Xu, W. *et al*. Graphene: A Platform for Surface-Enhanced Raman Spectroscopy. *Small* **9**, 1206-1224 (2013).
34. Yu, X. *et al*. Tuning Chemical Enhancement of SERS by Controlling the Chemical Reduction of Graphene Oxide Nanosheets. *ACS Nano* **5**, 952-958 (2011).
35. Gurunathan, S. *et al*. Enhanced green fluorescent protein-mediated synthesis of biocompatible graphene. *J. Nanobiotechnol.* **12**, 16 (2014).
36. Kumar, S. & Koh, J. Physiochemical and optical properties of chitosan based graphene oxide bionanocomposite. *Int. J. Biol. Macromol.* **70**, 559-564 (2014).
37. Park, J.S. *et al*. Mechanism of DNA Adsorption and Desorption on Graphene Oxide. *Langmuir* **30**, 12587-12595 (2014).
38. Park, J.S. *et al*. Desorption of single-stranded nucleic acids from graphene oxide by disruption of hydrogen bonding. *Analyst* **138**, 1745-1749 (2013).
39. Ramasamy, M.S. *et al*. Soluble conducting polymer-functionalized graphene oxide for air-operable actuator fabrication. *J. Mater. Chem. A* **2**, 4788-4794 (2014).

40. Gurunathan, S. *et al*. Green synthesis of graphene and its cytotoxic effects in human breast cancer cells. *Int. J. Nanomed*. **8**, 1015-1027 (2013).
41. Yadav, S.K. *et al*. Click coupled graphene for fabrication of high-performance polymer nanocomposites. *J. Polym. Sci. Pt. B-Polym. Phys*. **51**, 39-47 (2013).
42. Gurunathan, S. *et al*. Green chemistry approach for the synthesis of biocompatible graphene. *Int. J. Nanomed*. **8**, 2719-2732 (2013).
43. Gurunathan, S. *et al*. Microbial reduction of graphene oxide by Escherichia coli: A green chemistry approach. *Colloid Surf. B-Biointerfaces* **102**, 772-777 (2013).
44. Gurunathan, S. *et al*. Biocompatibility of microbially reduced graphene oxide in primary mouse embryonic fibroblast cells. *Colloid Surf. B-Biointerfaces* **105**, 58-66 (2013).
45. Gurunathan, S. *et al*. Humanin: A novel functional molecule for the green synthesis of graphene. *Colloid Surf. B-Biointerfaces* **111**, 376-383 (2013).
46. Kim, M.G. *et al*. Double stranded aptamer-anchored reduced graphene oxide as target-specific nano detector. *Biomaterials* **35**, 2999-3004 (2014).
47. Yun, Y.J. *et al*. A 3D scaffold for ultra-sensitive reduced graphene oxide gas sensors. *Nanoscale* **6**, 6511-6514 (2014).
48. Liu, X. *et al*. Functionalizing Metal Nanostructured Film with Graphene Oxide for Ultrasensitive Detection of Aromatic Molecules by Surface-Enhanced Raman Spectroscopy. *ACS Appl. Mater. Interfaces* **3**, 2944-2952 (2011).
49. Xu, W. *et al*. Surface enhanced Raman spectroscopy on a flat graphene surface. *Proc. Natl. Acad. Sci. U. S. A.* **109**, 9281-9286 (2012).
50. Xu, W. *et al*. Graphene-Veiled Gold Substrate for Surface-Enhanced Raman Spectroscopy. *Adv. Mater.* **25**, 928-933 (2013).
51. Kim, Y.-K. *et al*. Graphene Oxide Sheath on Ag Nanoparticle/Graphene Hybrid Films as an Antioxidative Coating and Enhancer of Surface-Enhanced Raman Scattering. *ACS Appl. Mater. Interfaces* **4**, 6545-6551 (2012).
52. Zhang, Z. *et al*. A facile one-pot method to high-quality Ag-graphene composite nanosheets for efficient surface-enhanced Raman scattering. *Chem. Commun*. **47**, 6440-6442 (2011).
53. Lu, G. *et al*. Surface enhanced Raman scattering of Ag or Au nanoparticle-decorated reduced graphene oxide for detection of aromatic molecules. *Chem. Sci*. **2**, 1817-1821 (2011).
54. Fan, W. *et al*. Graphene oxide and shape-controlled silver nanoparticle hybrids for ultrasensitive single-particle surface-enhanced Raman scattering (SERS) sensing. *Nanoscale* **6**, 4843-4851 (2014).
55. Hui, K.S. *et al*. Green synthesis of dimension-controlled silver nanoparticle-graphene oxide with in situ ultrasonication. *Acta Mater.* **64**, 326-332 (2014).
56. Shen, J. *et al*. Polyelectrolyte-assisted one-step hydrothermal synthesis of Ag-reduced graphene oxide composite and its antibacterial properties. *Mater Sci. Eng. C. Mater Biol. Appl*. **32**, 2042-2047 (2012).
57. Zhang, W.L. & Choi, H.J. Silica-Graphene Oxide Hybrid Composite Particles and Their Electroresponsive Characteristics. *Langmuir* **28**, 7055-7062 (2012).
58. Verma, S. *et al*. Graphene oxide: an efficient and reusable carbocatalyst for aza-Michael addition of amines to activated alkenes. *Chem. Commun*. **47**, 12673-12675 (2011).
59. Su, C.-Y. *et al*. Electrical and Spectroscopic Characterizations of Ultra-Large Reduced Graphene Oxide Monolayers. *Chem. Mater.* **21**, 5674-5680 (2009).
60. Michota, A. & Bukowska, J. Surface-enhanced Raman scattering (SERS) of 4-mercaptobenzoic acid on silver and gold substrates. *J. Raman Spectrosc*. **34**, 21-25 (2003).
61. Wang, F. *et al*. Surface-Enhanced Raman Scattering Detection of pH with Silica-Encapsulated 4-Mercaptobenzoic Acid-Functionalized Silver Nanoparticles. *Anal. Chem*. **84**, 8013-8019 (2012).
62. Zheng, J. *et al*. Surface-Enhanced Raman Scattering of 4-Aminothiophenol in Assemblies of Nanosized Particles and the Macroscopic Surface of Silver. *Langmuir* **19**, 632-636 (2003).
63. Anema, J.R. *et al*. Shell-Isolated Nanoparticle-Enhanced Raman Spectroscopy: Expanding the Versatility of Surface-Enhanced Raman Scattering. *Annu. Rev. Anal. Chem*. **4**, 129-150 (2011).
64. Kim, H.-M. *et al*. Large scale synthesis of surface-enhanced Raman scattering nanoprobes with high reproducibility and long-term stability. *J. Ind. Eng. Chem*. **33**, 22-27 (2016).
65. Kang, H. *et al*. One-step synthesis of silver nanoshells with bumps for highly sensitive near-IR SERS nanoprobes. *J. Mater. Chem. B* **2**, 4415-4421 (2014).

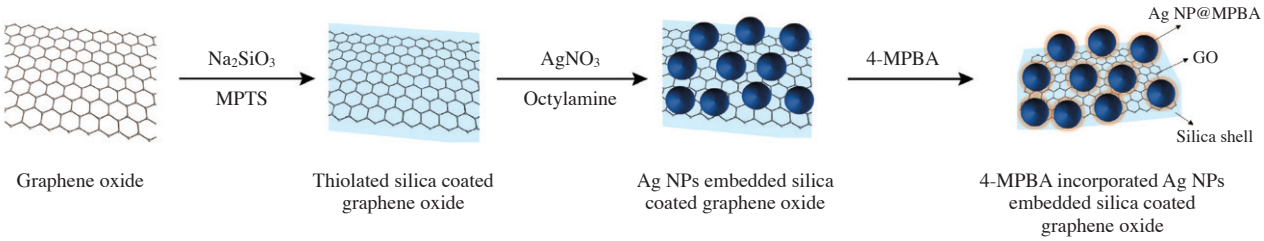

Figure S1. Fabrication process of silver nanoparticles embedded silica coated graphene oxide (GO@SiO_2@Ag NPs).

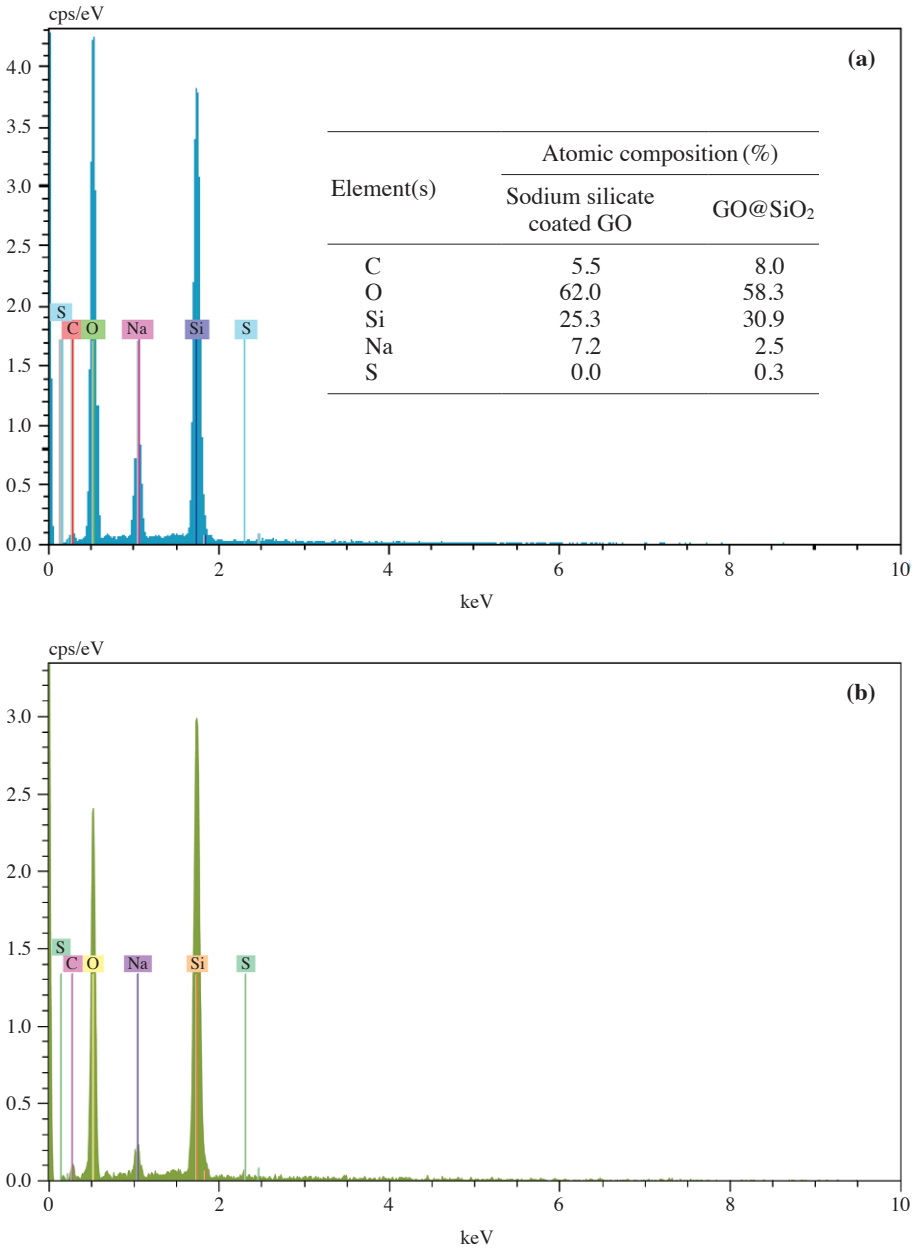

Element(s)	Atomic composition (%)	
	Sodium silicate coated GO	GO@SiO_2
C	5.5	8.0
O	62.0	58.3
Si	25.3	30.9
Na	7.2	2.5
S	0.0	0.3

Figure S2. EDX data of (a) sodium silicate coated graphene oxide and 3-mercaptopropyl trimethoxysilane coated graphene oxide (GO@SiO_2).

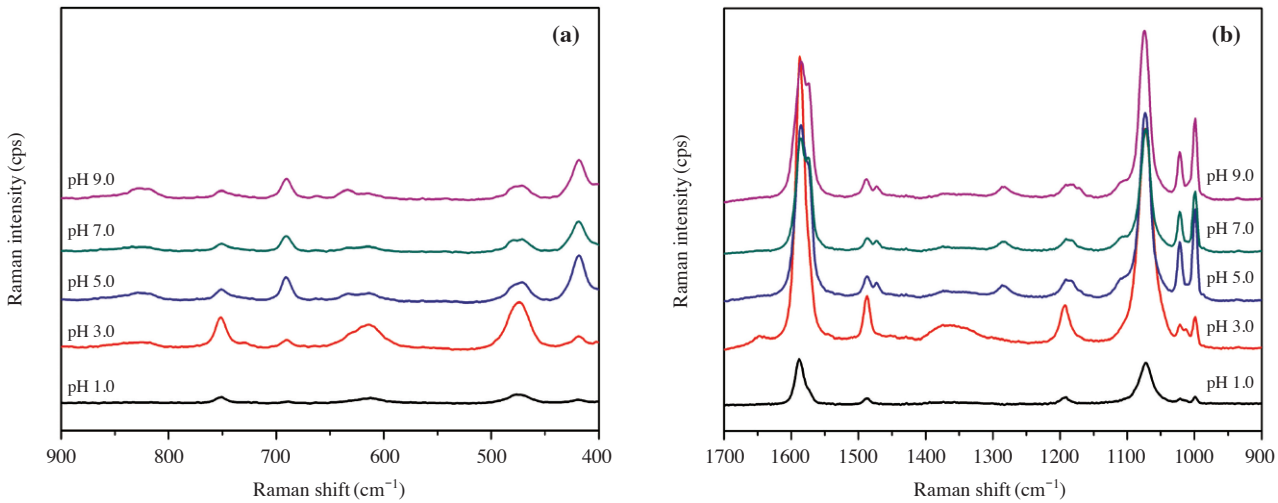

Figure S3. SERS intensity of 4-MPBA incorporated GO@SiO_2@Ag NPs in PBS at various pH solution in the absence of 5 mM glucose. GO concentration was 1 mg/mL, laser power was 10 mW, wavelength was 532 nm, integration time was 5 s, and laser spot was 2 μm.

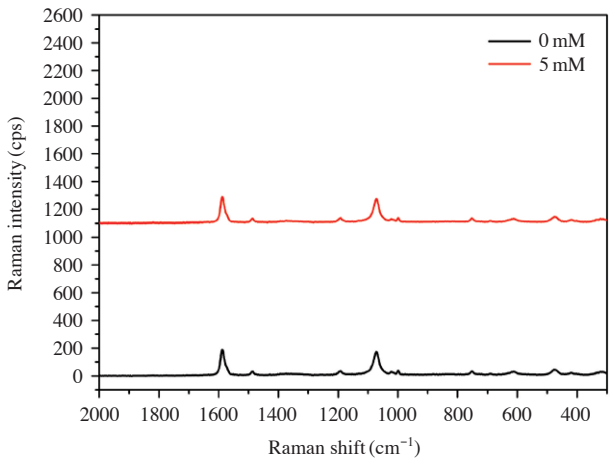

Figure S4. SERS intensity of 4-MPBA incorporated GO@SiO_2@Ag NPs in PBS pH 1.0 in the absence and presence of 5 mM glucose. GO concentration was 1 mg/mL, laser power was 10 mW, wavelength was 532 nm, integration time was 5 s, and laser spot was 2 μm.

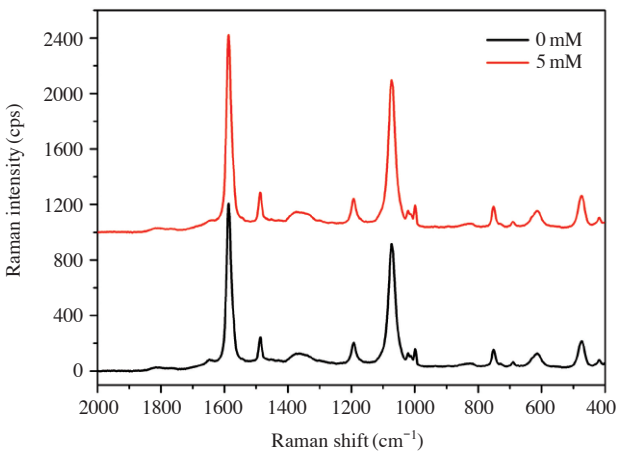

Figure S5. SERS intensity of 4-MPBA incorporated GO@SiO_2@Ag NPs in PBS pH 3.0 in the absence and presence of 5 mM glucose. GO concentration was 1 mg/mL, laser power was 10 mW, wavelength was 532 nm, integration time was 5 s, and laser spot was 2 μm.

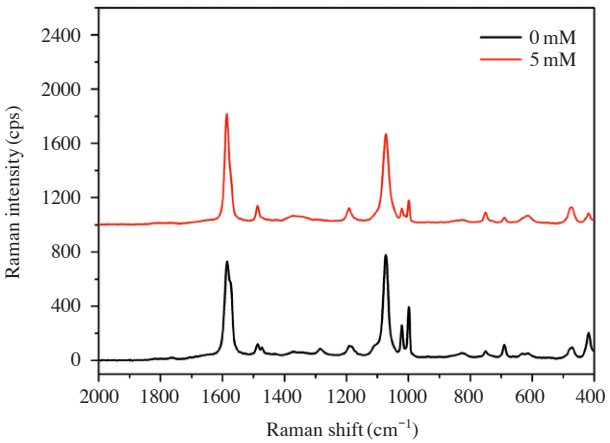

Figure S6. SERS intensity of 4-MPBA incorporated GO@SiO_2@Ag NPs in PBS pH 5.0 in the absence and presence of 5 mM glucose. GO concentration was 1 mg/mL, laser power was 10 mW, wavelength was 532 nm, integration time was 5 s, and laser spot was 2 μm.

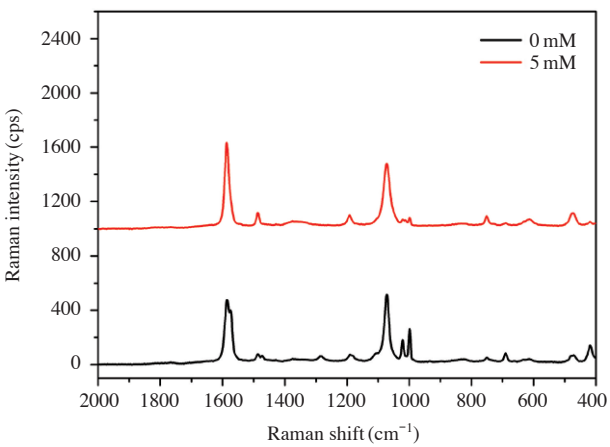

Figure S7. SERS intensity of 4-MPBA incorporated GO@SiO_2@Ag NPs in PBS pH 7.0 in the absence and presence of 5 mM glucose. GO concentration was 1 mg/mL, laser power was 10 mW, wavelength was 532 nm, integration time was 5 s, and laser spot was 2 μm.

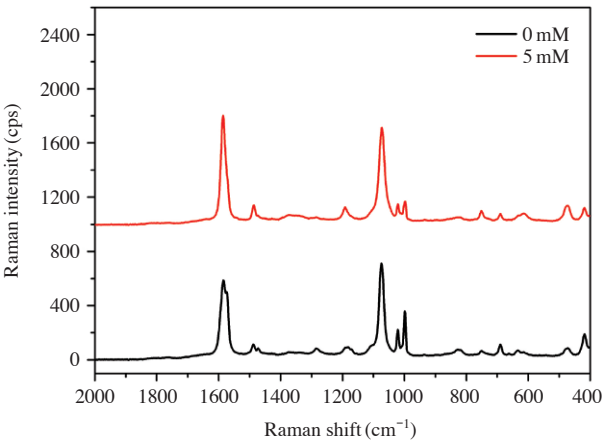

Figure S8. SERS intensity of 4-MPBA incorporated GO@SiO_2@Ag NPs in PBS pH 9.0 in the absence and presence of 5 mM glucose. GO concentration was 1 mg/mL, laser power was 10 mW, wavelength was 532 nm, integration time was 5 s, and laser spot was 2 μm.

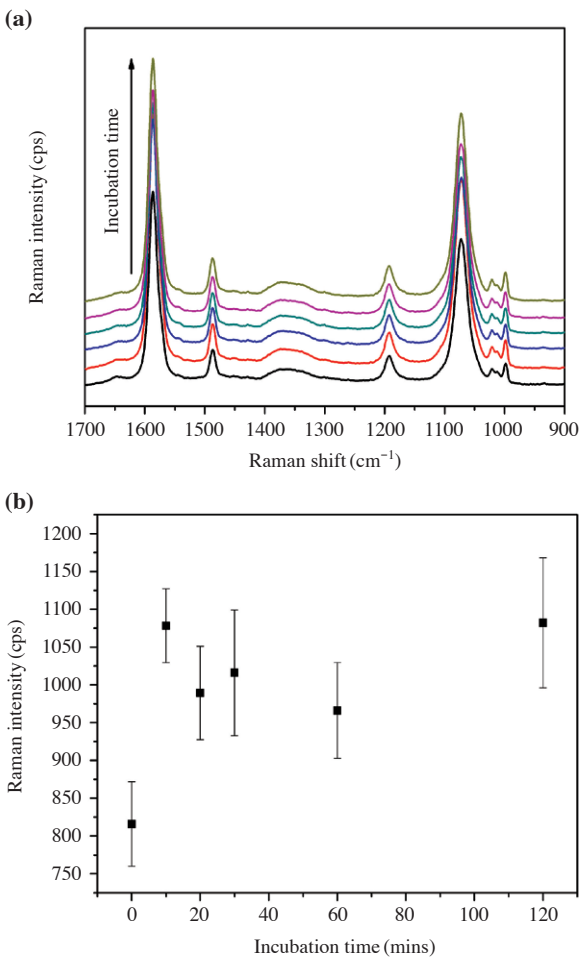

Figure S9. SERS spectra of 4-MPBA incorporated GO@SiO_2@Ag NPs in the presence of 5 mM glucose in pH 3.0 at various incubation times: 0, 10, 20, 30, 60, 120 mins.